Progress In Electromagnetics Research Letters, Vol. 104, 113–120, 2022

Toward the Development of an Efficient and Stability-Improved FDTD Method for Anisotropic Magnetized Plasma

Jian-Yun Gao[1] and Xiang-Hua Wang[2, *]

Abstract—An efficient and stability-improved finite-difference time-domain (FDTD) method with auxiliary difference equations (ADE) for cold magnetized plasma is developed in this paper. The two equations of Ampere's law and the auxiliary equation for plasma are unified as a single equation at first. Then the leapfrog difference scheme is applied to it and Faraday's law, respectively. By introducing a mid-term computation into the unified equation, the iterative equations of the ADE-FDTD for plasma are derived. Its stability condition remains the same as that of a vacuum which is analyzed and numerically verified. Numerical experiments show that our proposed method is more efficient than those provided by others but with the same accuracy. Finally, the transmission properties of a magnetized plasmonic slab are investigated. The reflection and transmission coefficients of the right-circularly-polarized (RCP) and left-circularly-polarized (LCP) waves are calculated. The results show that our proposed method can be applied to study these plasma-based structures accurately and efficiently.

1. INTRODUCTION

Based on directly discretizing Maxwell's equations, the finite-difference time-domain (FDTD) method is a powerful full-wave numerical method to simulate various materials, including plasma [1, 2]. As a dispersive media, there are generally two approaches to incorporating the plasma into Maxwell's curl equations. One way is that: first, directly convert the relation of the electric flux density **D** with the electric field intensity **E** from the frequency domain into the time domain; then, different types of time-domain iterative equations are developed, such as the recursive convolution FDTD (RC-FDTD) [3] and its extended piecewise-linear recursive convolution FDTD (PLRC-FDTD) [4]. The other approach is that: first, introduce an auxiliary equation (AE) characterized by the polarization current density **J** or the polarization intensity **P** to describe the effect of the plasma; then, a different type of discretizing method is applied to the AE to obtain its iterative equations, such as the **JE** convolution FDTD (JEC-FDTD) [5] and the auxiliary differential equation FDTD (ADE-FDTD) [6, 7]. Generally, the FDTD methods obtained by the first approach are more complicated. Their stability conditions are also hard to be analyzed. By directly discretizing the AE with a finite difference approximation, the ADE-FDTD is a simple but effective method. Therefore, it has been extensively studied recently. The ADE-FDTD methods related to **J** can be further divided into two categories with **HJ**- or **EJ**-collocated in the time domain. In [8], one simple HJ-ADE-FDTD was proposed. However, we found that compared with that for vacuum, the maximum timestep for plasma was reduced, i.e., its stability condition depends on the parameters of plasma. To overcome this drawback, the HJ-ADE-FDTD method with two timesteps was developed in [9]. It was further extended in [10]. However, they are more complicated than that in [8]. In addition, the EJ-ADE-FDTD method was proposed in [11]. Its stability condition is not related

Received 2 April 2022, Accepted 25 May 2022, Scheduled 6 June 2022

* Corresponding author: Xiang-Hua Wang (xhwang199@outlook.com).

[1] Department of Basic Courses, Tianjin Vocational Institute, Tianjin 300410, China. [2] School of Science, Tianjin University of Technology and Education, Tianjin 300222, China.

to the plasma's parameters. However, its iterative equations are complicated and inefficient for real applications. Therefore, it is necessary to develop one FDTD method with simple iterative equations and the stability condition not depending on the plasma's parameters.

In this paper, based on the methods provided in [8] and [11], we develop a new ADE-FDTD which is more efficient than those in [8] and [11] but keeps the stability condition being free of the plasma's parameters as that in [11].

2. METHODOLOGY

Maxwell's curl equations and the coupled polarization current density equations for anisotropic magnetized cold plasma can be written as:

$$\frac{\partial \mathbf{H}}{\partial t} = -\frac{1}{\mu_0}\nabla \times \mathbf{E} \tag{1a}$$

$$\frac{\partial \mathbf{E}}{\partial t} = \frac{1}{\varepsilon_0}(\nabla \times \mathbf{H} - \mathbf{J}) \tag{1b}$$

$$\frac{d\mathbf{J}}{dt} = \varepsilon_0 \omega_p^2 \mathbf{E} - \nu \mathbf{J} + \boldsymbol{\omega}_c \times \mathbf{J} \tag{1c}$$

where ν is the electron collision frequency, ω_p the plasma frequency, and $\boldsymbol{\omega}_c$ the plasma gyrofrequency with $\boldsymbol{\omega}_c = \omega_{cx} i + \omega_{cy} j + \omega_{cz} k$; here i, j, and k are the unit vectors along the x, y, and z-directions, respectively. To obtain a more unified form equation, (1b) and (1c) can be rewritten as:

$$\frac{\partial}{\partial t}\begin{pmatrix} \mathbf{E} \\ \mathbf{J} \end{pmatrix} = \begin{pmatrix} 0 & -1/\varepsilon_0 \\ \varepsilon_0 \omega_p^2 & -\nu + \boldsymbol{\omega}_c \times \end{pmatrix}\begin{pmatrix} \mathbf{E} \\ \mathbf{J} \end{pmatrix} + \begin{pmatrix} \nabla \times \mathbf{H}/\varepsilon_0 \\ 0 \end{pmatrix} \tag{2}$$

Further, we apply the time domain leapfrog scheme to (1a) and (2). The magnetic field $\mathbf{H}$ is sampled at $(n+1/2)\Delta t$ where n and Δt are the time index and time step increment, respectively. Its iterative equation from $\mathbf{H}^{n1/2}$ to $\mathbf{H}^{n+1/2}$ can be obtained from (1a) by using the central difference at $n\Delta t$:

$$\mathbf{H}^{n+1/2} = \mathbf{H}^{n-1/2} - \frac{\Delta t}{\mu_0}\nabla \times \mathbf{E}^n \tag{3}$$

$\mathbf{E}$ and $\mathbf{J}$ are set time collocated, and both are sampled at $n\Delta t$. To obtain iterative equations from $n\Delta t$ to $(n+1)\Delta t$, we split (2) into two substep calculations, i.e., sub-step#1:

$$\frac{1}{2}\frac{\partial}{\partial t}\begin{pmatrix} \mathbf{E} \\ \mathbf{J} \end{pmatrix} = \begin{pmatrix} 0 & -1/\varepsilon_0 \\ \varepsilon_0 \omega_p^2 & -\nu \end{pmatrix}\begin{pmatrix} \mathbf{E} \\ \mathbf{J} \end{pmatrix} + \begin{pmatrix} \nabla \times \mathbf{H}/\varepsilon_0 \\ 0 \end{pmatrix} \tag{4}$$

for $n\Delta t$ to $(n+1/2)\Delta t$; sub-step#2: for $(n+1/2)\Delta t$ to $n\Delta t$ by

$$\frac{1}{2}\frac{\partial}{\partial t}\begin{pmatrix} \mathbf{E} \\ \mathbf{J} \end{pmatrix} = \begin{pmatrix} 0 & 0 \\ 0 & \boldsymbol{\omega}_c \times \end{pmatrix}\begin{pmatrix} \mathbf{E} \\ \mathbf{J} \end{pmatrix} \tag{5}$$

It should be noted that we make a split field implementation to improve the efficiency where the isotropic properties are calculated in the first sub-step by (4), and the anisotropic effects are computed in the second sub-step by (5). Also note that Δt is the time increment from time index n to $n+1$.

Further, by applying the central difference to (4) at $(n+1/4)\Delta t$ and (5) at $(n+3/4)\Delta t$, with some mathematic manipulations, we have:

$$\mathbf{E}^{n+1/2} = \mathbf{E}^n + \frac{\Delta t}{\varepsilon_0}\nabla \times \mathbf{H}^{n+1/4} - \frac{\Delta t}{2\varepsilon_0}\left(\mathbf{J}^{n+1/2} + \mathbf{J}^n\right) \tag{6a}$$

$$\mathbf{J}^{n+1/2} = \frac{2-\nu\Delta t}{2+\nu\Delta t}\mathbf{J}^n + \frac{\varepsilon_0 \omega_p^2 \Delta t}{2+\nu\Delta t}\left(\mathbf{E}^{n+1/2} + \mathbf{E}^n\right) \tag{6b}$$

$$\mathbf{E}^{n+1} = \mathbf{E}^{n+1/2} \tag{6c}$$

$$\mathbf{J}^{n+1} = \mathbf{J}^{n+1/2} + \frac{\Delta t}{2}\boldsymbol{\omega}_c \times \left(\mathbf{J}^{n+1} + \mathbf{J}^{n+1/2}\right) \tag{6d}$$

From (6a), it can be seen that $\mathbf{H}^{n+1/4}$ is unknown, and it must be approximated by the known magnetic field. For simplicity, we directly set $\mathbf{H}^{n+1/4} = \mathbf{H}^{n+1/2}$. First substituting (6c) into (6a) and (6b), then (6b) into (6a), we can obtain the explicit iterative equation for $\mathbf{E}$ from $n\Delta t$ to $(n+1)\Delta t$ as:

$$\mathbf{E}^{n+1} = \frac{4+2\nu\Delta t-\Delta t^2\omega_p^2}{4+2\nu\Delta t+\Delta t^2\omega_p^2}\mathbf{E}^n + \frac{4\Delta t-2\nu\Delta t^2}{\varepsilon_0\left(4+2\nu\Delta t+\Delta t^2\omega_p^2\right)}\nabla\times\mathbf{H}^{n+1/2} - \frac{4\Delta t}{\varepsilon_0\left(4+2\nu\Delta t+\Delta t^2\omega_p^2\right)}\mathbf{J}^n \quad (7)$$

Substituting (6c) into (6b), we can obtain the explicit iterative equation for $\mathbf{J}$ from $n\Delta t$ to $(n+1/2)\Delta t$ as:

$$\mathbf{J}^{n+1/2} = \frac{2-\nu\Delta t}{2+\nu\Delta t}\mathbf{J}^n + \frac{\varepsilon_0\omega_p^2\Delta t}{2+\nu\Delta t}\left(\mathbf{E}^{n+1}+\mathbf{E}^n\right) \quad (8)$$

Note that (3), (6d), (7), and (8) are the iterative equations of our proposed method for magnetized plasma. We can see that only $\mathbf{J}$ is calculated twice within one time step. Therefore, our proposed method is more efficient than that provided in [11]. Moreover, the stability condition remains the same as that of conventional FDTD in free space which will be checked in the next sections. For clarity, the x component iterative equations can be derived as:

$$H_x^{n+1/2} = H_x^{n-1/2} - \frac{\Delta t}{\mu_0}\left(\frac{\partial E_z^n}{\partial y} - \frac{\partial E_y^n}{\partial z}\right) \quad (9a)$$

$$E_x^{n+1} = \frac{4+2\nu\Delta t-\Delta t^2\omega_p^2}{4+2\nu\Delta t+\Delta t^2\omega_p^2}E_x^n + \frac{4\Delta t-2\nu\Delta t^2}{\varepsilon_0\left(4+2\nu\Delta t+\Delta t^2\omega_p^2\right)}\left(\frac{\partial H_z^{n+1/2}}{\partial y} - \frac{\partial H_y^{n+1/2}}{\partial z}\right) - \frac{4\Delta t}{\varepsilon_0\left(4+2\nu\Delta t+\Delta t^2\omega_p^2\right)}J_x^n \quad (9b)$$

$$J_x^{n+1/2} = \frac{2-\nu\Delta t}{2+\nu\Delta t}J_x^n + \frac{\varepsilon_0\omega_p^2\Delta t}{2+\nu\Delta t}\left(E_x^{n+1}+E_x^n\right) \quad (9c)$$

$$J_x^{n+1} = \frac{4+\Delta t^2\left(\omega_{cx}^2-\omega_{cy}^2-\omega_{cz}^2\right)}{4+\Delta t^2\left(\omega_{cx}^2+\omega_{cy}^2+\omega_{cz}^2\right)}J_x^{n+1/2} + \frac{2\Delta t^2\omega_{cx}\omega_{cy}-4\Delta t\omega_{cz}}{4+\Delta t^2\left(\omega_{cx}^2+\omega_{cy}^2+\omega_{cz}^2\right)}J_y^{n+1/2} + \frac{2\Delta t^2\omega_{cx}\omega_{cz}+4\Delta t\omega_{cy}}{4+\Delta t^2\left(\omega_{cx}^2+\omega_{cy}^2+\omega_{cz}^2\right)}J_z^{n+1/2} \quad (9d)$$

Other equations can be obtained by circulating the notations of x, y, and z. Note that only second-order central difference in space is considered in the next studies. Therefore, when calculating $J_x|_{i+1/2,j,k}^{n+1}$ with (9d), $J_y|_{i+1/2,j,k}^{n+1/2}$ and $J_z|_{i+1/2,j,k}^{n+1/2}$ should be approximated by their neighbors in Yee's grids by:

$$J_y\Big|_{i+1/2,j,k}^{n+1/2} = \left(J_y\Big|_{i,j+1/2,k}^{n+1/2} + J_y\Big|_{i,j-1/2,k}^{n+1/2} + J_y\Big|_{i+1,j+1/2,k}^{n+1/2} + J_y\Big|_{i+1,j-1/2,k}^{n+1/2}\right)/4 \quad (10a)$$

$$J_z\Big|_{i+1/2,j,k}^{n+1/2} = \left(J_z\Big|_{i,j,k+1/2}^{n+1/2} + J_z\Big|_{i+1,j,k+1/2}^{n+1/2} + J_z\Big|_{i+1,j,k-1/2}^{n+1/2} + J_z\Big|_{i,j,k-1/2}^{n+1/2}\right)/4 \quad (10b)$$

3. STABILITY CONDITION

The stability condition is analyzed by using the Fourier method as described in [12]. In it, first, transforming the field components in Yee's grids [1] from space to a spatial-spectral domain, e.g.,

$$E_x\Big|_{i+1/2,j,k}^{n+1} = E_{0x}^{n+1}e^{-I(k_x(i+1/2)\Delta x+k_y j\Delta y+k_z k\Delta y)} \quad (11)$$

here I is the imaginary unit; k_x, k_y, and k_z are the wavenumbers along the x, y, and z-directions, respectively. Then, substituting (11) into (10) and the iterative equations of other components, after

some mathematic derivations, we have

$$\left(E_{0x}^{n+1}, E_{0y}^{n+1}, E_{0z}^{n+1}, J_{0x}^{n+1}, J_{0y}^{n+1}, J_{0z}^{n+1}, H_{0x}^{n+1/2}, H_{0y}^{n+1/2}, H_{0z}^{n+1/2}\right)^T$$
$$= \mathbf{M}_{9\times 9}\left(E_{0x}^{n}, E_{0y}^{n}, E_{0z}^{n}, J_{0x}^{n}, J_{0y}^{n}, J_{0z}^{n}, H_{0x}^{n-1/2}, H_{0y}^{n-1/2}, H_{0z}^{n-1/2}\right)^T \quad (12)$$

here $\mathbf{M}_{9\times 9}$ is the growing matrix, and its detailed expression is not given here for space limitation. If the proposed method is stable, all the eigenvalues should remain on or within the unit circle. Because it is difficult even impossible to work out all the eigenvalues and give a theoretical analysis, we check the stability condition by exhaustive numerical experiments with an extensive selection of the grid sizes, time steps, and the plasm's parameters. As known, to meet the stability condition of conventional second-order FDTD for free space, the maximum time step is $\Delta t_{FDTD} = 1/(c_0\sqrt{1/\Delta x^2 + 1/\Delta y^2 + 1/\Delta z^2})$ where c_0 is the speed of light in free space [1]. In the experiments, we set $\Delta t = \Delta t_{FDTD}$, $\Delta x = \Delta y = \Delta z = \Delta = 5 \times 10^{-5}$ m, $k_x = \cos(\theta)\cos(\varphi)$, $k_y = \cos(\theta)\sin(\varphi)$, $k_z = \sin(\theta)$, $\theta = [0, 180°]$ with $\Delta\theta = 30°$, $\varphi = [0, 360°]$ with $\Delta\varphi = 60°$, the plasma's parameters: $\omega_p = 10^{np}$ Hz with $np = [1, 20]$ and $\Delta np = 1$, $\omega_{cx} = \omega_{cy} = \omega_{cz} = 1^{nc}$ Hz with $nc = [1, 20]$ and $\Delta np = 1$, $\nu = 10^{n\nu}$ Hz with $n\nu = [1, 20]$ and $\Delta n\nu = 1$. The calculated eigenvalues are given in Figure 1. It can be seen that all of them are on or within the unit circle. Therefore, for the selected parameters, the stability condition proposed method for plasma remains the same as that of FDTD for free space.

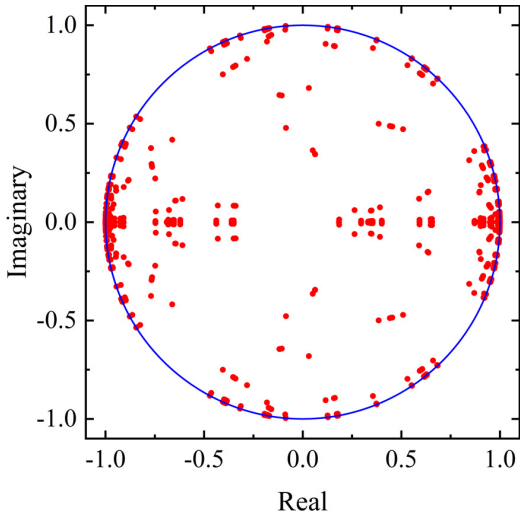

Figure 1. Eigenvalues of growing matrix by an extensive selection of plasma parameters.

4. STABILITY AND EFFICIENCY INVESTIGATIONS

To check the stability and efficiency, a cubic PEC cavity with half-space plasma filled is calculated as depicted in Figure 2. In the numerical experiments, we set $\Delta x = \Delta y = \Delta z = \Delta = 5 \times 10^{-5}$ m the edge length of the cavity $L = 40\Delta$, $\Delta t = \Delta t_{FDTD} = \Delta/(c_0\sqrt{3})$, $\omega_p = 10^{13}$ Hz, $\omega_{cx} = \omega_{cy} = \omega_{cz} = 10^{11}$ Hz, $\nu = 1^{13}$ Hz. A line current source, with the form of $J(t) = e^{-4\pi(t-t_0)^2/\tau^2}$ here $t_0 = \tau = 200\Delta t$, located from back to forth and 2Δ above the cavity center, is used to excite the electromagnetic field. We define CFLN $= \Delta t/\Delta t_{FDTD}$ (CFLN, Courant-Friedrich-Levy (CFL) Number [1]) as the parameter to check the stability condition. The field observation point is set at 9Δ away from the line current center along the y-direction.

Figure 2 shows the observed E_x computed by the proposed method with CFLN $= 1$. For comparison, the results computed by the methods provided in [11] with CFLN $= 1$ and [8] with CFLN $= 0.901$ and 0.903 are also given. The total time step is set as $1247\Delta t_{FDTD} \approx 0.12$ ns in all the simulations. We can see that the recorded field computed by the proposed method is almost

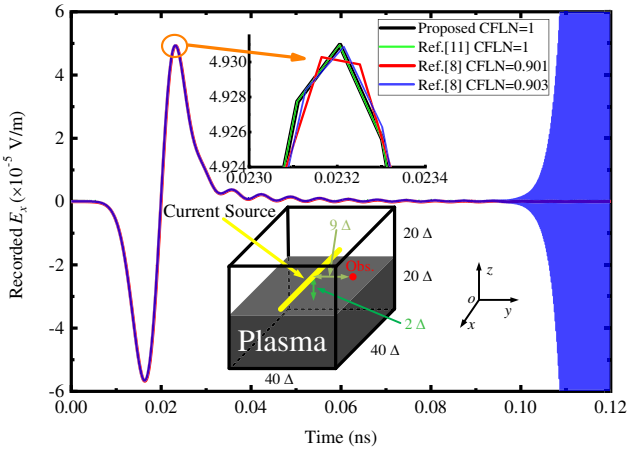

Figure 2. Recorded E_x computed by the proposed FDTD and that provided in [11] with CFLN = 1. The results computed by the method in [8] with CFLN = 0.901 and 0.903 are also given for comparison.

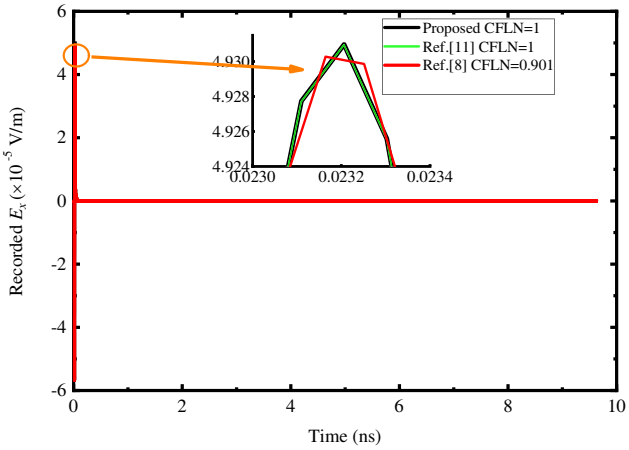

Figure 3. Recorded E_x computed with a large simulation total time step.

the same as that by [11]. Both of them agree well with that computed by [8] with CFLN = 0.901. It should be noted that, as discussed in [13], the maximum CFLN of the method provided in [8] is $\text{CFLN}_{\max} = 1/\sqrt{1+(\omega_p \Delta t_{FDTD}/2)^2} = 0.901$. As expected, when we choose a slightly larger CFLN e.g., 0.903, the field goes to infinity with the increase of time.

To further check the stability and efficiency, we run the simulations with a large total time step i.e., $10^5 \Delta t_{FDTD} \approx 9.6$ ns. Figure 3 shows the recorded E_x computed with CFLN = 1 and those provided in [8] with CFLN = 1 and in [11] with CFLN = 0.901. It is seen that our proposed method is always stable. Therefore, we may conclude that compared with the method provided in [8], our proposed method is stability-improved; the stability condition of our proposed method, being the same as that provided in [11], is not plasma's parameters dependent. As for the consumptions of total simulation times, they are 55.5 s, 63.43 s, and 97.2 s for our proposed method, that provided in [8], and that provided in [11], respectively. The simulation platform is a ThinkPad PC with CPU Intel i9-10885H 2.4 GHz and RAM 128 GB, Win10 OS, and Intel Fortran compiler. We can see that our proposed method is the most efficient. To make a further comparison, the update equation for E_x provided in [11] is given as:

$$E_x^{n+1} = c_1 E_x^n + c_2 E_y^n + c_3 E_z^n + c_4 J_x^n + c_5 J_y^n + c_6 J_z^n + c_7 \left(\frac{\partial H_x^{n+1/2}}{\partial z} - \frac{\partial H_z^{n+1/2}}{\partial x} \right) + c_8 \left(\frac{\partial H_y^{n+1/2}}{\partial x} - \frac{\partial H_x^{n+1/2}}{\partial y} \right) + c_9 \left(\frac{\partial H_z^{n+1/2}}{\partial y} - \frac{\partial H_y^{n+1/2}}{\partial z} \right) \quad (13)$$

where for the parameters we set $c_1 = 0.729407$, $c_2 = 0.758275 \times 10^{-3}$, $c_3 = -0762549 \times 10^{-3}$, $c_4 = -0634760 \times 10^{-2}$, $c_5 = 0.177877 \times 10^{-4}$, $c_6 = -0178879 \times 10^{-4}$, $c_7 = 0.412322 \times 10^{-5}$, $c_8 = -0414646 \times 10^{-5}$, $c_9 = 0.940388 \times 10^{-2}$.

From (9b), we have:

$$E_x^{n+1} = 0.729402 \cdot E_x^n - 0.634770 \times 10^{-2} \cdot J_x^n + 0.940386 \times 10^{-2} \cdot \left(\frac{\partial H_z^{n+1/2}}{\partial y} - \frac{\partial H_y^{n+1/2}}{\partial z} \right) \quad (14)$$

Comparing (13) with (14), it is obvious that our proposed method is more concise and efficient. Moreover, because a reduced CFLN must be chosen when the method provided in [8] is used, the total simulation time of [8] is larger than our proposed method. Therefore, our proposed method can be used to efficiently investigate the practical problems with complex plasmonic structures.

5. ACCURACY AND APPLICATIONS

To check the accuracy, the reflection and transmission characteristics of a magnetized plasma slab are investigated. This structure is chosen because its analytical results exist. As depicted in Figure 4, the total simulation domain is $20\Delta \times 20\Delta \times 420\Delta$ including a 200Δ thick plasma slab where $\Delta = \Delta x = \Delta y = \Delta z = 5 \times 10^{-5}$ m. The plasma's parameters are set as $\omega_p = 2 \times 10^{11}$ Hz, $\omega_{cx} = 0$, $\omega_{cy} = 0$, $\omega_{cz} = 10^{11}$ Hz, $\nu = 10^{10}$ Hz. The total field/scattered field boundary (TF/SF) is applied to excite the electromagnetic field with a Gaussian current pulse $J_x(t) = e^{-4\pi(t-t_0)^2/\tau^2}$ where $t_0 = \tau = 200\Delta t$. Two observation points are set above and under the slab to record the fields which are used to calculate the reflection and transmission coefficients. 10-layer convolutional perfectly matched layers (CPML) [14] are used to absorb the outgoing EM fields. The periodic boundary condition (PBC) is set in the x and y-directions to model an infinitely wide plasma slab.

The right circularly polarized (RCP) and left circularly polarized (LCP) reflection and transmission

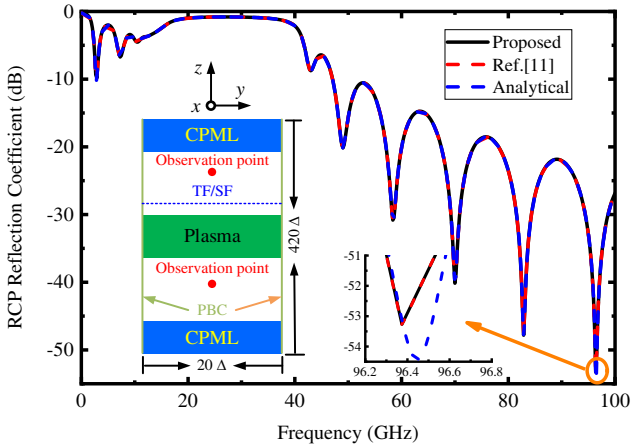

Figure 4. The computed RCP reflection coefficient. The results of analytical and calculated with [11] are also given for comparison.

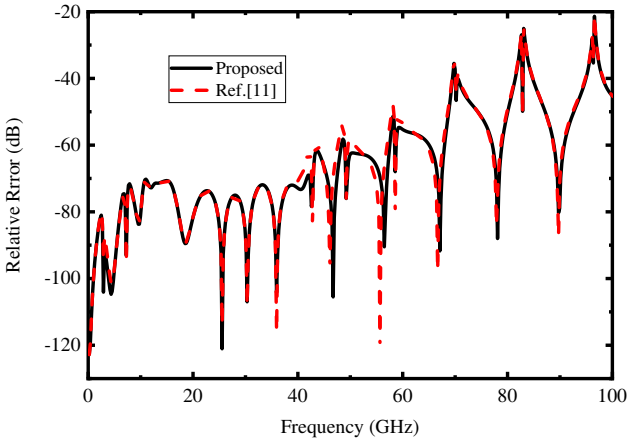

Figure 5. The relative error of our proposed method. For comparison, the result computed by the method provided in [11] is also given.

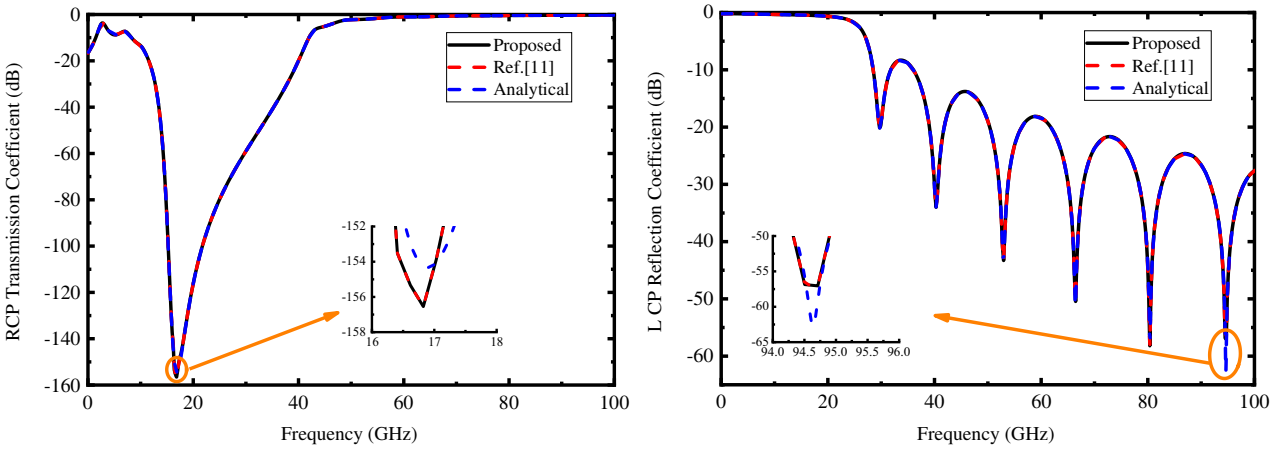

(a) (b)

Figure 6. The computed RCP transmission coefficient and LCP reflection coefficient.

coefficients are computed by using the recorded fields at the observation points with [15]:

$$R_{RCP}(f), T_{RCP}(f) = 20\log_{10}\left(\frac{|FFT(E_{x,obs}(t)) + jFFT(E_{y,obs}(t))|}{|FFT(E_{x,inc}(t))|}\right) \tag{15a}$$

$$R_{LCP}(f), T_{LCP}(f) = 20\log_{10}\left(\frac{|FFT(E_{x,obs}(t)) - jFFT(E_{y,obs}(t))|}{|FFT(E_{x,inc}(t))|}\right) \tag{15b}$$

where FFT means the fast Fourier transformation. Figure 4 shows the RCL reflection coefficient computed by the proposed method. For comparison, the results of analytical [16] and computed by the method provided in [11] are also given. It is seen that both the simulated lines are in good agreement with the analytical one. To check the accuracy, the relative errors are calculated as in Figure 5. we can see that the relative error of our proposed method is almost the same as that provided in [11]. To further investigate the accuracy, the RCP transmission and LCP reflection coefficients are also computed as in Figure 6. It is seen that they all agree well. Therefore, from all the investigations above, we may conclude that our proposed method is more efficient than the methods provided in [8] and [11] while keeping the same accuracy as the method provided in [11].

6. CONCLUSION

A new EJ collocated FDTD method for magnetized plasma has been developed in this paper. With only the split field implementation for the current density, our proposed method is more efficient and stability-improved than the methods provided by others while keeping its high accuracy. Therefore, the proposed method can be applied to investigate the magnetized plasma-based structures efficiently and accurately.

REFERENCES

1. Taflove, A. and S. C. Hagness, *Computational Electromagnetics: Finite-Difference Time-Domain Method*, 3rd Edition, Artech House, Norwood, MA, 2005.
2. Teixeira, F. L., "Time-domain finite-difference and finite-element methods for Maxwell equations in complex media," *IEEE Trans. Antennas Propag.*, Vol. 56, No. 8, 2150–2166, 2008.
3. Luebbers, R. J., F. Hunsberger, and K. S. Kunz, "A frequency-dependent finite-difference time-domain formulation for transient propagation in plasma," *IEEE Trans. Antennas Propag.*, Vol. 39, No. 1, 29–34, 1991.
4. Xu, L. and N. Yuan, "FDTD formulations for scattering from 3-D anisotropic magnetized plasma objects," *IEEE Antennas Wireless Propag. Lett.*, Vol. 5, 335–338, 2006.
5. Zhang, J., H. Fu, and W. Scales, "FDTD analysis of propagation and absorption in nonuniform anisotropic magnetized plasma slab," *IEEE Trans. Plasma Sci.*, Vol. 46, No. 6, 2146–2153, 2018.
6. Young, J. L., A. Kittichartphayak, Y. M. Kwok, and D. Sullivan, "On the dispersion errors related to $(FD)^2TD$ type schemes," *IEEE Trans. Microw. Theory Tech.*, Vol. 43, No. 8, 1902–1909, 1995.
7. Surkova, M., W. Tierens, I. Pavlenko, D. Van Eester, G. Van Oost, and D. De Zutter, "3-D discrete dispersion relation, numerical stability, and accuracy of the hybrid FDTD model for cold magnetized toroidal plasma," *IEEE Trans. Antennas Propag.*, Vol. 62, No. 12, 6307–6316, 2014.
8. Liu, S. B., J. J. Mo, and N. C. Yuan, "An auxiliary differential equation FDTD method for anisotropic magnetized plasma," *Acta Physica Sinica*, Vol. 53. No. 7, 2233–2236, 2004.
9. Samimi, A. and J. J. Simpson, "An efficient 3-D FDTD model of electromagnetic wave propagation in magnetized plasma," *IEEE Trans. Antennas Propag.*, Vol. 63, No. 1, 269–279, 2015.
10. Pokhrel, S., V. Shankar, and J. J. Simpson, "3-D FDTD modeling of electromagnetic wave propagation in magnetized plasma requiring singular updates to the current density equation," *IEEE Trans. Antennas Propag.*, Vol. 66, No. 9, 4772–4781, 2018.
11. Yu, Y. and J. J. Simpson, "An E-J collocated 3-D FDTD model of electromagnetic wave propagation in magnetized cold plasma," *IEEE Trans. Antennas Propag.*, Vol. 58, No. 2, 469–478, 2010.

12. Smith, G. D., *Numerical Solution of Partial Differential Equations*, Oxford Univ. Press, Oxford, U.K., 1978.
13. Roden, J. A. and S. D. Gedney, "Convolutional PML (CPML): An efficient FDTD implementation of the CFS PML for arbitrary media," *Microw. Opt. Tech. Lett.*, Vol. 50, 334–339, 2000.
14. Hu, W. and S. A. Cummer, "An FDTD model for low and high altitude lightning-generated EM fields," *IEEE Trans. Antennas Propag.*, Vol. 54, No. 5, 1513–1522, 2006.
15. Hunsberger, F., R. Luebbers, and K. Kunz, "Finite-difference time-domain analysis of gyrotropic media. I. Magnetized plasma," *IEEE Trans. Antennas Propag.*, Vol. 40, No. 12, 1489–1495, 1992.
16. Balanis, C., *Advanced Engineering Electromagnetics*, Wiley, New York, 1989.